

## IMPEDANCE-MISMATCHED HYPERLENS WITH INCREASING LAYER THICKNESSES

X. Li<sup>1,\*</sup>, Y. Q. Ye<sup>1</sup>, and Y. Jin<sup>2</sup>

<sup>1</sup>Department of Physics and Institute of Condensed Matter Physics, Hangzhou Normal University, Hangzhou 310012, China

<sup>2</sup>Centre for Optical and Electromagnetic Research, Zhejiang University; Joint Research Center of Photonics of the Royal Institute of Technology (Sweden) and Zhejiang University, Zijingang Campus, Hangzhou 310058, China

**Abstract**—Structure with non-negative effective permittivities in the radial and tangential directions can also perform far-field imaging beyond the diffraction limit since the dispersion curves can be long and flat enough and utilized to transfer the subwavelength information. Thus we propose an impedance-mismatched hyperlens with such a dispersion curve and increasing thicknesses (from the innermost layer to the outermost) to reduce reflection losses due to the impedance difference between the nearby layer pairs. Compared with the hyperlens with same thickness for each period, the resolution ability of the hyperlens with varying thicknesses can be improved dramatically, while the image intensity is weaker. Furthermore, the influence of the layer number on the imaging is also analyzed to improve the performance of the system and an improved hyperlens with repeated thickness setting is also utilized to increase the intensity of the magnified image.

### 1. INTRODUCTION

A conventional imaging system only transforms propagating components, and loses the decaying evanescent waves when detected in the far field. In the previous research, different regimes and methods based on the simple layered structures are suggested to improve the subwavelength image in the near-field zone [1–5] and recently in the far-field zone [6]. Such structures amplify partial evanescent waves but still

---

*Received 20 April 2011, Accepted 27 June 2011, Scheduled 5 July 2011*

\* Corresponding author: Xuan Li (lixuan.zju@gmail.com).

keep their decaying character and thus near field detection is required. Recently, Jacob et al. suggested a novel structure called hyperlens [7], based on strongly anisotropic metamaterials of cylindrical geometry. It can magnify a subwavelength object and project the image into the far field. This extraordinary concept confirmed first by experimental demonstration in [8]. Such a device would convert evanescent waves to propagating waves and make the detection and processing easier. The hyperlens is composed of a (half) cylinder metamaterials with opposite signs of the permittivity in the radial and tangential directions, and has strongly hyperbolic dispersion for the TM-polarized waves. Thus in principle it enables nearly all the spatial harmonics (including evanescent components) of the source radiation to be transformed into propagating harmonics within the structure. As a result, the diffraction limit of conventional optics can be beaten by such a structure. Although the hyperlens which is composed of a (half) cylinder metamaterials is different from the multilayered structures, the imaging mechanism and parameters setting (e.g., permittivities) for subwavelength focusing (especially for multilayered system) in the previous research [9–13] will provide a lot of prospective and help for our current research in hyperlens. Moreover, systematical research on the cylindrical structure [14, 15] and novel design approaches on the hyperlens (mainly on the impedance matched cases) [16–18] will also provide a lot of help and guidance.

In the present paper, we will study another kind of hyperlens structure with mismatched impedance, which has different dispersion relation with the above strongly hyperbolic dispersion relation, to improve the quality of the far-field imaging. Besides the approximate expressions [7] for the effective permittivities in the radial and tangential directions, to render a reliable analysis, we will use more accurate expressions for the effective permittivities to adjust the parameter setting of the system. Thus the local permittivities for the neighboring layer pair (one positive and one negative permittivity layers) in tangential and radial directions can be kept constant as the radial distance varies. We expect to achieve better magnification performance using such an improved structure.

## 2. DISPERSION CURVES OF THE HYPERLENS WITH UNIAXIAL ANISOTROPY

In the case of uniaxial anisotropy, dielectric permittivity is characterized by two parameters:  $\varepsilon_r$  along the optical axis of the structure, and  $\varepsilon_\theta$  transverse to the optical axis. Propagating modes can be decomposed into two polarization states: the TE and TM waves.

In the present paper we only consider the TM waves (i.e., the electric field vector has components both along and transverse to the optical axis). The dispersion relation given by

$$\frac{k_r^2}{\varepsilon_\theta} + \frac{k_\theta^2}{\varepsilon_r} = k_0^2 \tag{1}$$

For the strong anisotropy considered in [7], where  $\varepsilon_r$  and  $\varepsilon_\theta$  are of opposite signs, the dispersion curve is hyperbolic with infinite-length. This medium is characterized without cut-off property. When the tangential permittivity  $\varepsilon_\theta = 0$  and radial permittivity  $\varepsilon_r = \infty$  (or a very large number, e.g., 1000), a flat infinite (or very long) dispersion curve can be obtained in the lossless case. Such cylindrical anisotropy can also make a high angular momentum state to penetrate toward the center (in isotropic dielectrics, high- $m$  modes cannot penetrate toward the center and carry no subwavelength information), and enables extra information channels for retrieving the object’s subwavelength details. The cylindrical TM mode solution for the above anisotropy is given by [7]

$$B_z \propto J_{m\sqrt{\varepsilon_r/\varepsilon_0}}\left(\frac{\omega}{c}\sqrt{\varepsilon_\theta}r\right) \exp(im\phi) \tag{2}$$

Figure 1 shows that such a cylindrical anisotropy with  $\varepsilon_\theta = 0$  and  $\varepsilon_r = 1000$  (very large value compared with  $\varepsilon_\theta = 0$ ) causes a high angular momentum state to penetrate toward the center. In [10], we found that the impedance match between the structures and air is not necessary for the subwavelength focusing based on the transmission device. Similarly,  $\varepsilon_\theta = 0$  is chosen here.

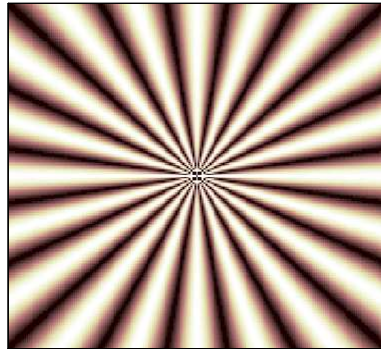


**Figure 1.** High angular momentum states ( $m = 20$ ) in a bulk metamaterial with  $\varepsilon_\theta = 0$  and  $\varepsilon_r = 1000$  (the regions of high intensity and low intensity are shown in black white, respectively).It shows a local section of the cylindrical anisotropy and the center is the center of the metamaterial. We can see that the field penetrates to the center.

The high angular momentum modes carry subwavelength information about the object. Our system with two non-negative permittivities allows some high angular momentums to participate in the imaging and we expect that such a system can magnify the subwavelength object. In the following, we will focus on using metamaterials to construct such a medium.

### 3. ORDINARY HYPERLENS WITH TWO NON-NEGATIVE EFFECTIVE PERMITTIVITIES

We now consider a hollow core cylinder consisting of alternating concentric layers with positive permittivity ( $\varepsilon_1$ ) and negative permittivity ( $\varepsilon_2$ ) (see Fig. 2) [7]. The source is placed inside the core of the hyperlens and the image will be formed outside the structure. The total layer number is  $2N$ . The inner and outer radii of the innermost layer (i.e., the 1th layer) are  $r_1$  and  $r_2$ , and those of the  $n$ th layer ( $1 \leq n \leq 2N$ ) are  $r_n$  and  $r_{n+1}$ , respectively.

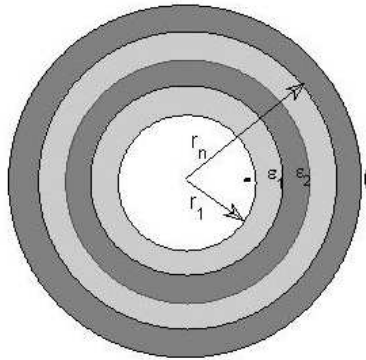


**Figure 2.** Top view of the hyperlens made of  $2N$  alternating layers of metal (dark regions) with  $\varepsilon_2$  and dielectric (grey regions) with  $\varepsilon_1$ .

For all  $n$ , thickness  $d_n = r_{n+1} - r_n$  of the  $n$ th layer is much smaller than the operating wavelength, and thus we can treat this finely structured material as an effective medium. As was demonstrated [19–22], the operating wavelength  $\lambda$  is chosen to be  $11 \mu\text{m}$ . SiC layers with  $\varepsilon_2 = -4 + 0.25i$  and SiO<sub>2</sub> layers with  $\varepsilon_1 = 4$  are utilized here as the negative and positive permittivity ones. In the optical frequencies, we can choose noble metal (e.g., gold. Drude model of gold agrees with the experimental data very well and we can use the model to calculate its permittivity at the operating frequency [23, 24]) to be the negative-permittivity material. Similar to the system in [7], the

total thickness of any two neighboring layers (as a period) is the same and equal to  $0.6 \mu\text{ m}$  (i.e., for odd  $n$ ,  $d_n = d_1$  and for even  $n$ ,  $d_n = d_2$ ) and we have approximate expressions for effective permittivities  $\tilde{\varepsilon}_\theta = (\varepsilon_1 d_1 + \varepsilon_2 d_2)/(d_1 + d_2)$  and  $\tilde{\varepsilon}_r = [(\varepsilon_1^{-1} d_1 + \varepsilon_2^{-1} d_2)/(d_1 + d_2)]^{-1}$ . Here for all  $n$ , we choose  $d_n = d/2 = 0.30 \mu\text{ m}$  at first. To reduce the attenuation of the evanescent wave in the free space, we put the point source near the inner air-hyperlens interface (the distance between them in the radius direction is much less than the level of  $r_1$  and layer thickness). First we choose  $N = 20$ .

In the present paper, we use the transfer matrix method [14] to compute the transmission coefficients for all the spatial harmonics radiated from the source to obtain the image of a point source (with infinite small size and infinite large peak intensity). The image plane here is a circle, and for convenience the image intensity is a function of radian here. In order to describe the focusing quality of a certain structure for the point source, here we utilize the Full Width at Half Maximum ( $FWHM'$ ) of the point source imaging as a function of radian (the unit of  $FWHM'$  is radian here and the ordinary unit of the FWHM is length). Thus the resolution ability of the hyperlens system for the subwavelength information can be defined as  $\overline{FWHM} = FWHM' \cdot r_1/\lambda$ . We can directly compare the value of  $\overline{FWHM}$  with the unit of 1 and smaller  $\overline{FWHM}$  represents a better magnification performance of the system for the point source. Besides, we define a parameter  $G_M$  which represents the peak value of the magnetic field intensity at the image (the peak value of the intensity distribution at the inner interface of the hyperlens is 5.65). From simulation (see Fig. 3),  $\overline{FWHM}$  of the system is 0.075,  $G_M = 0.0147$  for the previous parameter setting. However, the reflection from the

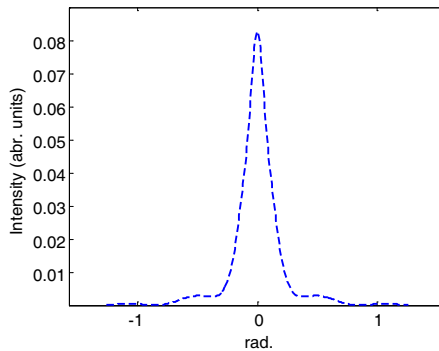


**Figure 3.** Magnetic intensity at the image plane for a point source when  $\lambda = 11 \mu\text{ m}$ ,  $\varepsilon_1 = 4$ ,  $\varepsilon_2 = -4 + 0.25i$  and the structure is composed of  $N = 20$  periods.

inner interface of the system is strong according to the simulation.

From Fig. 3, it can be found that multilayered cylindrical structures with  $\varepsilon_1 = 4$ ,  $\varepsilon_2 = -4 + 0.25i$  and suitable layer thickness can be utilized to magnify the point source with subwavelength dimension. The disadvantage of this structure is that the reflection from the interface of the system is strong because of the impedance mismatch. According to the previous research results [4, 5, 10], we can adjust the total thickness of the structure to satisfy Fabry-Perot resonance effect and finally achieve good image. Besides, it is understandable that a structure with a smaller effective index (i.e., permittivity  $\varepsilon_\theta$  here) corresponding to a larger effective wavelength has a larger displacement range, i.e., less sensitive to some small deviation of the layer positions.

#### 4. THE IMPROVED HYPERLENS WITH MORE STABLE EFFECTIVE PERMITTIVITIES

In Ref. [25], a cylindrical metal annulus is suggested to behave like a lens. In this paper, a hollow core cylinder consisting of two concentric layers of negative-permittivity ( $\varepsilon_1$ ) and positive permittivity ( $\varepsilon_2$ ) materials is considered in the near field limit first (the center locate at origin; the radii of three circular interfaces from inside out are  $r_1$ ,  $r_2$  and  $r_3$ , respectively). A line dipole with charges  $\pm q$  locates in the hollow core cylinder (one charge at origin and the other at distance  $a_1$  from the origin.) will produce different potential distribution. Matching the potential across the three boundaries and we can get the expressions for the potential of the outside space (here we are mainly concerned about the potential of the outside space):

$$\phi = \frac{-q}{2\pi\varepsilon_0} \sum_{m=1}^{\infty} C_m^- r^{-m} \cos m\theta \quad (3)$$

where  $C_m^- = \frac{a_1^m 4\varepsilon_0\varepsilon_1}{mr_1^{2m}((\varepsilon_1+\varepsilon_0)^2 r_2^{-2m} - (\varepsilon_1-\varepsilon_0)^2 r_3^{-2m} r_1^{-2m}/r_2^{-2m})}$  as  $\varepsilon_1 = -\varepsilon_2$ . When  $r_3 r_1 = r_2^2$ , we can get  $C_m^- = a_1^m r_2^{2m}/(m r_1^{2m})$  and the expression for potential  $\phi$  of the outside space can be written as

$$\phi = \frac{-q}{2\pi\varepsilon_0} \sum_{m=1}^{\infty} \frac{a_2^{-m}}{m r^m} \cos m\theta \quad (4)$$

where  $a_2 = a_1(r_2/r_1)^2 = a_1(r_3/r_1)$ . The system behaves like a lens magnifying the dipole with size  $r_1$  and the magnification factor equals to  $r_3/r_1$ . If we assume  $r_1 = a_1$ , we can get  $a_2 = r_3$  where  $r_3/r_2 = r_2/r_1$ . Thus we know that for such a cylindrical annulus lens structure, the thicknesses for the two neighboring layers are different. Moreover, we

will also place the source close to the inner air-hyperlens interface to let more evanescent components of the source transformed into the structure and it can be considered that the image plane locates at the outer air-hyperlens interface. Based on this result, we will study the parameter setting for a multilayered hyperlens.

The effective medium theory can give good guidance and description of certain structure's optical behavior. For the multilayered structure with the same period parameters, we can get that for every neighboring layer pair (i.e.,  $n = 1, 2, \dots, 2N - 1$ ) the permittivity expressions  $(\varepsilon_n d_n + \varepsilon_{n+1} d_{n+1}) / (d_n + d_{n+1})$  equals to  $(\varepsilon_1 d_1 + \varepsilon_2 d_2) / (d_1 + d_2)$  and  $[(\varepsilon_n^{-1} d_n + \varepsilon_{n+1}^{-1} d_{n+1}) / (d_n + d_{n+1})]^{-1}$  equal to  $[(\varepsilon_1^{-1} d_1 + \varepsilon_2^{-1} d_2) / (d_1 + d_2)]^{-1}$  based on the transmission line model in [4] and therefore  $(\varepsilon_1 d_1 + \varepsilon_2 d_2) / (d_1 + d_2)$  and  $[(\varepsilon_1^{-1} d_1 + \varepsilon_2^{-1} d_2) / (d_1 + d_2)]^{-1}$  can represent the effective permittivities in the direction parallel and normal in Cartesian coordinate system. But for the multilayered hyperlens structure, different layer has different radius and therefore each cylindrical layer is different. Similar to the transmission line model in [4], we can deduce the two parameters  $\varepsilon_\theta^{n,n+1}$  and  $\varepsilon_r^{n,n+1}$  related to the local permittivities for the two neighboring layers (the  $n$ th and  $n + 1$ th layers,  $1 \leq n < 2N$ ) in the radial and tangential directions in cylindrical coordinates. The expressions can be obtained as follows:

$$\varepsilon_r^{n,n+1} = \ln\left(\frac{r_{n+2}}{r_n}\right) / \left( \frac{\ln(r_{n+2})}{\varepsilon_{n+1}} - \frac{\ln(r_n)}{\varepsilon_n} + \left(\frac{1}{\varepsilon_n} - \frac{1}{\varepsilon_{n+1}}\right) \ln(r_{n+1}) \right); \quad (5a)$$

$$\varepsilon_\theta^{n,n+1} = \left( \varepsilon_n \ln\left(\frac{r_{n+1}}{r_n}\right) + \varepsilon_{n+1} \ln\left(\frac{r_{n+2}}{r_{n+1}}\right) \right) / \ln\left(\frac{r_{n+2}}{r_n}\right) \quad (5b)$$

where  $\varepsilon_n$  is the positive permittivity  $\varepsilon_1$  as  $n$  is odd otherwise  $\varepsilon_n$  is the negative permittivity  $\varepsilon_2$  and  $\ln(x)$  is the natural logarithm of  $x$ . When the thickness of every period is the same, as  $r_n \rightarrow \infty$  (i.e.,  $n \rightarrow \infty$ ), Eq. (5) becomes  $\varepsilon_r^\infty = 2\varepsilon_n \varepsilon_{n+1} / (\varepsilon_n + \varepsilon_{n+1})$  and  $\varepsilon_\theta^\infty = (\varepsilon_n + \varepsilon_{n+1}) / 2$ . Thus  $\varepsilon_r^\infty$  and  $\varepsilon_\theta^\infty$  are only the approximate effective nonzero diagonal components of the anisotropic permittivity tensor. As  $n$  increases to infinite the value of  $\varepsilon_\theta^{n,n+1}$  and  $\varepsilon_r^{n,n+1}$  keep oscillating before converging to  $\varepsilon_r^\infty$  and  $\varepsilon_\theta^\infty$  (i.e., the amplitude of oscillation monotonically decreases). Based on the effective medium theory, if we can keep the values of  $\varepsilon_r^{n,n+1}$  and  $\varepsilon_\theta^{n,n+1}$  unchanged as  $n$  varies, reflection within the structure will be reduced and the performance of the system may be improved. In the practical design, the layer number should not be too large because of the material loss and  $r_1$  can not be too large due to the magnifying property (approximately described by  $r_{2N} / r_1$ , this value should be large enough, e.g., 10) of the hyperlens.

We try to utilize different parameter setting (e.g., different layer thicknesses) to keep  $\varepsilon_\theta^{n,n+1}$  and  $\varepsilon_r^{n,n+1}$  unchanged for all  $n$  so that effective permittivities will be the local permittivities in Eq. (5). It can be found that if  $r_{n+2}/r_{n+1} = r_{n+1}/r_n \equiv c$  ( $1 \leq n < 2N$  and  $c$  is a constant), Eq. (5) becomes

$$\begin{aligned}\varepsilon_r^{n,n+1} &= \varepsilon_r(r_{n+2}/r_{n+1} = r_{n+1}/r_n \equiv c) = \frac{2\varepsilon_n\varepsilon_{n+1}}{\varepsilon_n + \varepsilon_{n+1}}; \\ \varepsilon_\theta^{n,n+1} &= \varepsilon_\theta = \frac{\varepsilon_n + \varepsilon_{n+1}}{2}\end{aligned}\quad (6)$$

Thus we propose an improved structure with different thickness for each layer. For all  $n$ ,  $d_n = r_{n+1} - r_n$  should be a positive value. Thus we obtain that the constant  $c$  in Eq. (6) should be larger than 1. The thickness of the  $n$ th layer can be written as  $d_n = (c-1)r_n$ . As  $n$  increases, the layer thickness  $d_n$  will also increase. Thus our improved structure consists of those concentric layers whose thicknesses are a monotonously increasing sequence. The maximal thickness  $d_{2N} = c^{2N-1}(c-1)r_1$  should be much smaller than the half wavelength, thus  $d_{2N}$  should satisfy  $d_{2N} < \lambda/B$  ( $B$  is a constant and can be chosen according to the practical request. E.g.,  $B$  could be 10). Thus we can obtain an approximate upper limit for the pair number  $N < N_{\max} = (\log_c(\lambda/(Br_1(c-1))) + 1)/2$ .

The resolution of the hyperlens is determined by the effective wavelength at the core and is given by  $\Delta \propto (r_{2N}/r_1)\lambda$  [7]. We can define magnification factor as  $A = r_{2N}/r_1$ , which is related to the magnifying ability of a hyperlens for the subwavelength source. For the ideal hyperlens, the source located at  $r = r_1$  and the image located at  $r = r_{2N}$  should have the same  $FWHM$ ' (i.e., light follows the radial direction). In the practical situation, light may be bent outwards (with respect to the radial direction, see Fig. 4(b)) because of the material loss or other reasons. Thus for imaging a point source with a practical hyperlens, smaller  $\overline{FWHM}$  represents a better performance of the hyperlens as the magnification factor is fixed.

In order to magnify smaller subwavelength information, the magnification factor  $A$  should be much larger than 1 (e.g.,  $A = 10$ ). Thus there is a lower limit for  $N$  and  $N > N_{\min} = \log(A)/\log(c^2)$ . Through selecting different values for  $c$ , we can get different value ranges for pair number  $N$ , e.g., if we choose  $c = 1.03$ ,  $B = 4$ ,  $r_1 = \lambda/2$  and  $A = 10$ , then the approximate limit value for  $N$  is  $N < 48$  and  $N > 39$ .

When  $c$  is chosen to be a larger value, both the upper and lower limits will decrease. Contrarily, they will increase. As  $r_1$  decreases, the upper limit  $N_{\max}$  will increase accordingly while the lower limit keeps

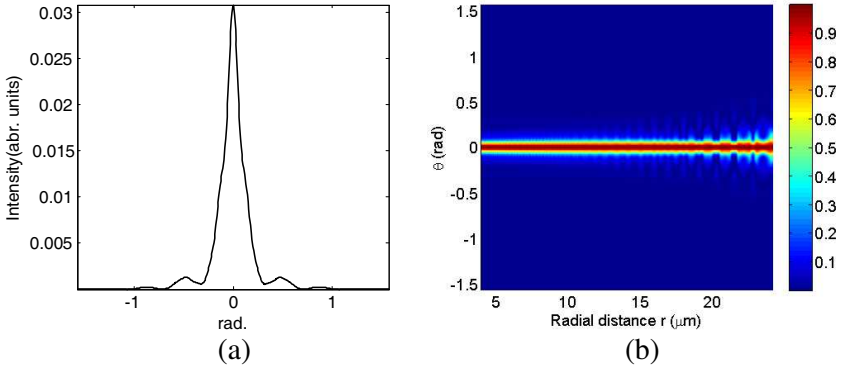


**Figure 4.** (a) Magnetic intensity at the image plane for a point source when  $\lambda = 11 \mu\text{m}$ ,  $\varepsilon_1 = 4$ ,  $\varepsilon_2 = -4 + 0.25i$  and the pair number of the structure is  $N = 30$ . (b) Corresponding relative intensity  $I_r$  as a function of distance  $r$  and angular  $\theta$ . At any fixed distance  $r$ , relative intensity  $I_r$  (as a function of  $\theta$ ) equals the magnetic field intensity (at distance  $r$ ) divided by the corresponding maximum intensity  $G_m(r)$  (the maximum intensity at distance  $r$  from the center). It shows the highly directional nature of the beam from the point sources.

unchanged. The lower limit  $N_{\text{min}}$  will decrease as  $A$  decreases. It is easy to know that a larger  $B$  corresponds to a smaller pair number (the outmost layer should be thinner).

Here we choose pair number  $N = 30$ ,  $c = 1.03$  and  $r_1 = 4$  as an example. The values of  $\overline{FWHM}$  and  $G_M$  ( $G_M$  is the maximum value of the magnetic intensity at the image plane for the point source and note that  $G_m(r)$  is the maximum value of the magnetic intensity at the distance  $r$  from the center) for such a system are 0.061 and 0.034, respectively. The reflection loss within the hyperlens system is smaller.

From the simulation, it can be seen that such an improved hyperlens structure has good far-field magnification performance for a subwavelength object. Thus not only an ordinary hyperlens but also the improved hyperlens (both have non-negative effective permittivities) has good performance when they magnify the subwavelength information, although the impedances of the two systems don't match with the surrounding air.

## 5. FAR-FIELD MAGNIFICATION IMAGING OF THE ORDINARY AND IMPROVED STRUCTURES

In this section, we will study two different far-field imaging structures both with mismatched impedance as the period number changes. One

is the ordinary hyperlens structure with the same thickness for each period, and the other is the improved hyperlens structure (i.e., each layer has different thickness). When we compare the performance of the two structures, they should have the same layer number  $N$ ,  $r_1$  and total thickness  $D$  (i.e., they have the same magnification factor  $A$ ). Parameter  $c$  of the improved hyperlens is chosen to be 1.03,  $A = 5$  and  $B = 5$ . Thus for our improved hyperlens the approximate upper and lower limits for pair number  $N$  are 49 and 27, respectively. The value range for  $N$  is from 25 to 51 (a little bit wider than the approximately calculated value range). According to the simulation, the  $\overline{FWHM}$  and  $G_M$  as functions of the system's total thickness for both the improved and ordinary hyperlenses are shown in Fig. 5.

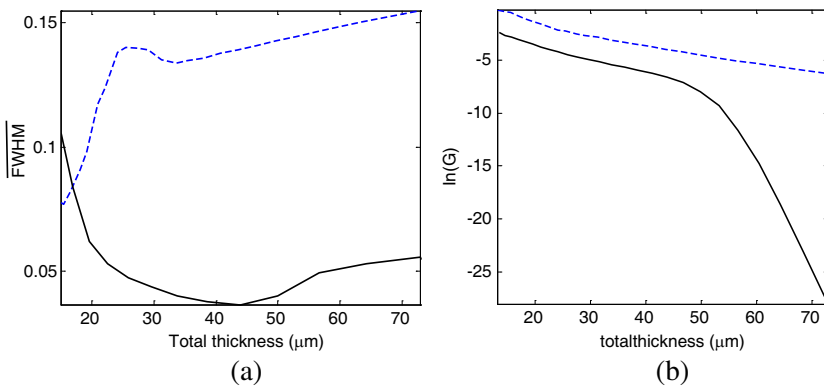


**Figure 5.** (a)  $\overline{FWHM}$  and (b)  $G_M$  as functions of the total thickness. The solid black curves are for the improved hyperlens and the dashed blue curves are for the ordinary hyperlens.

In Fig. 5, one can see that  $\overline{FWHM}$  of the improved hyperlens is smaller than that of the ordinary hyperlens in most cases. For the improved hyperlens, the  $\overline{FWHM}$  decreases at first and then increases as the total thickness increases. As  $N$  decreases close to the lower limit or increase close to the upper limit, the  $\overline{FWHM}$  will increase and the resolution will be degraded. This is consistent with our approximate limit for the pair number  $N$ . According to Fig. 5(b), we'd better choose pair number  $N$  smaller than 45 (i.e., the total thickness is smaller than 52 μm) in the practical design of the improved hyperlens. When  $N = 43$  (i.e., the total thickness is 45.2 μm), the minimum  $\overline{FWHM} = 0.0364$  is obtained.

From the simulation, it can be found that the performance of the thick ordinary hyperlens is not as good as those with very small

total thickness (i.e., considering the  $\overline{FWHM}$  and image intensity). However, the magnification factor  $A$  of thin structure is small and this means the magnifying ability of the system is also weak. Some subwavelength information is still of subwavelength size after magnification and the near field detection is still needed. This doesn't satisfy the design intention of a hyperlens.

For both hyperlenses, the image intensity decreases exponentially as the total thickness increases because of material losses. The total thickness of the structures cannot be too large. Otherwise, the image intensity is too weak to be detected. When the pair number is close to or larger than the upper limit, the image is too bad for both systems. For the improved structure, although the  $\overline{FWHM}$  is still good, the image intensity is too weak. For the ordinary structure, the image intensity is acceptable but the  $\overline{FWHM}$  is dramatically degraded. Compared with the ordinary hyperlens, the improved structure produces much weaker image intensity which may lead to detection difficulty in applications. This is due to the fact that the outer layers (especially the outermost layer) are much thicker than those of the ordinary hyperlens. We know that, in order to resist material loss and improve subwavelength imaging, Pendry and Ramakrishna [26] cut one thick metal slab into many thin layers and separated them (i.e., alternative metal and air layers). Thus in the present improved structure, the presence of thick layers leads to some disadvantages (i.e., weak image intensity) of such a system. We can design a new improved structure with repeated thickness setting (we separate all the layers into 2 groups). When  $1 \leq n \leq N'$  (where  $N' = N$  when  $N$  is even and  $N' = N + 1$  when  $N$  is odd),  $d_n = c^n r_1 - c^{n-1} r_1$  and when  $n > N'$ ,  $d_n = d_{n-N'}$ . Thus the thickest layers of this new structure would not be too thick and the image intensity may increase. We compare the imaging property of the new improved structure and the ordinary structure. From simulation, for a new improved structure with  $c = 1.04$  and  $N = 40$ ,  $\overline{FWHM}$  is 0.042 and  $G_M = 1.4 \times 10^{-3}$ . For an ordinary structure with a fixed period but the same total thickness and pair number  $\overline{FWHM}$  is 0.049 and  $G_M = 0.58 \times 10^{-3}$ . It can easily be found that  $\overline{FWHM}$  and the magnetic field intensity of the former is better than those of the latter. However, in Fig. 5(b), we can see that the  $G_M$  of the improved hyperlens is much smaller than that of the ordinary hyperlens. We can obtain that this new design for the improved hyperlens help to increase the magnetic intensity of the image. Thus in the practical applications our new improved hyperlens may achieve good resolution and acceptable image intensity at the same time when the parameters of the hyperlens are carefully chosen.

## 6. CONCLUSION

In present paper, an improved hyperlens with layers of geometrically growing thickness is demonstrated to project an image to the far field beyond the diffraction limit. Our system possesses non-negative effective permittivities in the tangential and radial directions and increases layer thicknesses from the innermost layer. Increasing thicknesses of the improved system can help to reduce reflection losses within the structure and finally improve the performance of the system. Besides, we have analyzed the influence of layer number on the imaging quality. Different parameters should be purposefully chosen for the improved hyperlens according to the practical requests and our research results can give a good guidance. A new improved hyperlens with repeated thickness setting is only briefly discussed and we found it can dramatically improve intensity of the imaging compared with the improved hyperlens. In the following study, we will study on utilizing different methods (e.g., separating all the layers into  $M$  groups ( $M > 2$ ) or adjusting the surface termination [22]) to optimize such kind of hyperlens in detail. Moreover, tunable hyperlens will be studied based on the different novel materials (e.g., composites of negative-permittivity particles) [27–29]. Such system can overcome some drawbacks of the structures from pure metals and can work for any desired wavelengths by just adjusting the volume fraction of negative-permittivity particles.

## ACKNOWLEDGMENT

This work is partly supported by the Swedish Research Council (VR) (No. 2006-4048), National Natural Science Foundations (NNSF) of China under project No. 10604046 and 61007032.

## REFERENCES

1. Pendry, J. B., “Negative refraction makes a perfect lens,” *Phys. Rev. Lett.*, Vol. 85, 3966–3969, 2000.
2. Fang, N., H. Lee, C. Sun, and X. Zhang, “Sub-diffraction-limited optical imaging with a silver superlens,” *Science*, Vol. 308, 534–537, 2005.
3. Ramakrishna, S. A., J. B. Pendry, M. C. K. Wiltshire, and W. J. Stewart, “Imaging the near field,” *J. Mod. Optics*, Vol. 50, 1419–1430, 2003.
4. Belov, P. A. and Y. Hao, “Subwavelength imaging at optical frequencies using a transmission device formed by a periodic

- layered metal-dielectric structure operating in the canalization regime,” *Phys. Rev. B*, Vol. 73, 113110, 2006.
5. Jin, Y., “Improving subwavelength resolution of multilayered structures containing negative-permittivity layers by flattening the transmission curves,” *Progress In Electromagnetics Research*, Vol. 105, 347–364, 2010.
  6. Cao, P., X. Zhang, L. Cheng, and Q. Meng, “Far field imaging research based on multilayer positive- and negative-refractive-index media under off-axis illumination,” *Progress In Electromagnetics Research*, Vol. 98, 283–298, 2009.
  7. Jacob, Z., L. V. Alekseyev, and E. Narimanov, “Optical hyperlens: Far-field imaging beyond the diffraction limit,” *Opt. Express*, Vol. 14, 8247–8256, 2006.
  8. Liu, Z., H. Lee, Y. Xiong, C. Sun, and X. Zhang, “Far-field optical hyperlens magnifying sub-diffraction-limited objects,” *Science*, Vol. 315, 1686, 2007.
  9. De Ceglia, D., M. A. Vincenti, M. G. Cappeddu, M. Centini, N. Akozbek, A. D’Orazio, J. W. Haus, M. J. Bloemer, and M. Scalora “Tailoring metallodielectric structures for superresolution and superguiding applications in the visible and near-ir ranges,” *Phys. Rev. A*, Vol. 77, 033848, 2008.
  10. Li, X., S. L. He, and Y. Jin, “Subwavelength focusing with a multilayered Fabry-Perot structure at optical frequencies,” *Phys. Rev. B*, Vol. 75, 045103, 2007.
  11. Luo, C., S. G. Johnson, and J. D. Joannopoulos, “All-angle negative refraction without negative effective index,” *Phys. Rev. B*, Vol. 65, 201104(R), 2002.
  12. Pustai, D. M., S. Shi, C. Chen, A. Sharkawy, and D. W. Prather, “Analysis of splitters for self-collimated beams in planar photonic crystals,” *Opt. Express*, Vol. 12, 1823–1831, 2004.
  13. Augustin, M., R. Iliw, C. Etrich, D. Schelle, H.-J. Fuchs, U. Peschel, S. Nolte, E.-B. Kley, F. Lederer, and A. Tünnermann, “Self-guiding of infrared and visible light in photonic crystal slabs,” *Appl. Phys. B*, Vol. 81, 313, 2005.
  14. Chew, W. C., *Waves and Fields in Inhomogeneous Media*, 161–182, Wiley-IEEE Press, 1999.
  15. Ahmed, S. and Q. A. Naqvi, “Directive EM radiation of a line source in the presence of a coated PEMC circular cylinder,” *Progress In Electromagnetics Research*, Vol. 92, 91–102, 2009.
  16. Kildishev, A. V. and E. E. Narimanov, “Impedance-matched hyperlens,” *Opt. Lett.*, Vol. 32, 3432–3434, 2007.

17. Jacob, Z., L. V. Alekseyev, and E. Narimanov, "Semiclassical theory of the hyperlens," *J. Opt. Soc. Am. A*, Vol. 24, 10, 2007.
18. Kildishev, A. V., U. K. Chettiar, Z. Jacob, V. M. Shalaev, and E. Narimanov, "Materializing a binary hyperlens design," *Appl. Phys. Lett.*, Vol. 94, 071102, 2009.
19. Shvets, G. and Y. Urzhumov, "Polariton-enhanced near field lithography and imaging with infrared light," *Mater. Res. Soc. Symp. Proc.*, Vol. 820, R1.2.1, 2004.
20. Korobkin, D., Y. Urzhumov, and G. Shvets, "Enhanced near-field resolution in midinfrared using metamaterials," *J. Opt. Soc. Am. B*, Vol. 23, 468–478, 2005.
21. Li, X., F. Zhuang, and C. V. Köhnenkamp, "Optimized effective permittivity to improve imaging resolution of multilayered structures in infrared," *J. Opt. Soc. Am. A*, Vol. 26, 365–370, 2009.
22. Li, X. and Y. Jin, "Appropriate interface termination to improve imaging resolution of multilayered structures in the infrared and optical canalization regime," *J. Opt. Soc. Am. A*, Vol. 24, 1861–1864, 2008.
23. Weber, M. J., *Handbook of Optical Materials*, CRC Press, New York, 2003.
24. Xie, H., F. Kong, and K. Li, "The electric field enhancement and resonance in optical antenna composed of Au nanoparticles," *Journal of Electromagnetic Waves and Applications*, Vol. 23, No. 4, 535–548, 2009.
25. Pendry, J. B. and S. A. Ramakrishna, "Near field lenses in two dimensions," *J. Phys., Condensed Matter*, Vol. 14, 1–17, 2002.
26. Pendry, J. B. and S. A. Ramakrishna, "Refining the perfect lens," *Physica B*, Vol. 338, 329–332, 2003.
27. Gao, D. and L. Gao, "Tunable lateral shift through nonlinear composites of nonspherical particles," *Progress In Electromagnetics Research*, Vol. 99, 273–287, 2009.
28. Li, X. and F. Zhuang, "The multilayered structures with high subwavelength resolution based on the metal-dielectric composites," *J. Opt. Soc. Am. A*, Vol. 26, 2521–2525, 2009.
29. Wu, C. J., J. J. Liao, and T. W. Chang, "Tunable multilayer Fabry-Perot resonator using electro-optical defect layer," *Journal of Electromagnetic Waves and Applications*, Vol. 24, No. 4, 531–542, 2010.